Journal of Alloys and Compounds 527 (2012) 84–89

Contents lists available at SciVerse ScienceDirect

Journal of Alloys and Compounds

journal homepage: www.elsevier.com/locate/jallcom

Elucidating the microwave dielectric properties of $(Mg_{(1-x)}Zn_x)_2SnO_4$ ceramics

Yih-Chien Chen*

Department of Electrical Engineering, Lunghwa University of Science and Technology, Gueishan Shiang, Taoyuan County, Taiwan

ARTICLE INFO

Article history:
Received 19 August 2011
Received in revised form 27 February 2012
Accepted 4 March 2012
Available online xxx

Keywords:
$(Mg_{0.93}Zn_{0.07})_2SnO_4$
X-ray diffraction pattern
Dielectric constant
Quality factor
Temperature coefficient of resonant frequency

ABSTRACT

The microwave dielectric properties of $(Mg_{(1-x)}Zn_x)_2SnO_4$ ceramics were examined with a view to their exploitation for mobile communication. The $(Mg_{(1-x)}Zn_x)_2SnO_4$ ceramics were prepared by the conventional solid-state method with various sintering temperatures. The X-ray diffraction patterns of the $(Mg_{0.93}Zn_{0.07})_2SnO_4$ ceramics revealed no significant variation of phase with sintering temperatures. Dielectric constant (ε_r) of 8.50, quality factor ($Q \times f$) of 186,100 GHz, and temperature coefficient of resonant frequency (τ_f) of −61 ppm/°C were obtained for $(Mg_{0.93}Zn_{0.07})_2SnO_4$ ceramics that were sintered at 1550 °C for 4 h.

1. Introduction

Materials that are to be used in microwave devices must have three dielectric characteristics – a high dielectric constant, a high quality factor, and a near-zero temperature coefficient of resonant frequency. These enable small devices with low loss and high temperature stability, respectively, to be fabricated [1,2]. However, the carrier frequencies of interest are from the ISM (industrial, scientific and medical) bands to values that correspond to millimeter wavelengths. Materials with low dielectric constants are being introduced to replace materials with high dielectric constants in the millimeter wave range.

Mg_2SnO_4 ceramics exhibit a dielectric constant of 8.41, a quality factor ($Q \times f$) of 55,100 GHz, and a temperature coefficient of resonant frequency (τ_f) of −62.0 ppm/°C when sintered at 1550 °C for 4 h [3]. Since the ionic radius of Zn^{2+} (0.074 nm) is similar to that of Mg^{2+} (0.072 nm), the Mg^{2+} ion can be replaced by with the Zn^{2+} ion to form $(Mg_{(1-x)}Zn_x)_2SnO_4$ [4]. In this investigation, $(Mg_{(1-x)}Zn_x)_2SnO_4$ were synthesized and some of the Mg^{2+} ions were substituted with Zn^{2+} ions to improve their microwave dielectric properties. Moreover, the effect of the sintering temperature on the microwave dielectric properties of $(Mg_{(1-x)}Zn_x)_2SnO_4$ ceramics was studied. $(Mg_{(1-x)}Zn_x)_2SnO_4$ ceramics were synthesized by the conventional mixed-oxide method and demonstrated to have better microwave dielectric properties than Mg_2SnO_4 ceramics. The microwave dielectric properties of $(Mg_{(1-x)}Zn_x)_2SnO_4$ ceramics were found to vary with the degrees of Zn^{2+} substitution and sintering temperatures. These various microwave dielectric properties were analyzed by densification, X-ray diffraction (XRD) patterns, and observation of their microstructures.

2. Experimental procedure

The starting raw chemicals were MgO (99.3%), ZnO (99.9%), and SnO_2 (99.0%) powders. The prepared compound was $(Mg_{(1-x)}Zn_x)_2SnO_4$. Specimens were prepared by the conventional mixed-oxide method. The raw material was weighed out in stoichiometric proportions, ball-milled in alcohol, dried, and then calcined at 1200 °C for 4 h. The calcined powder was re-milled for 12 h using PVA solution as a binder. The obtained powder was then crushed into a fine powder through a sieve with a 200 mesh. The obtained fine powder was then axially pressed at 2000 kg/cm^2 into pellets with a diameter of 11 mm and a thickness of 6 mm. The specimens thus obtained were then sintered at temperatures of 1450–1600 °C for 4 h in air. Both the heating rate and the cooling rate were set to 10 °C/min. Following sintering, the phases of the samples were investigated by X-ray diffraction. X-ray Rigaku D/MAX-2200 spectrometer was used with Cu Kα radiation (at 30 kV and 20 mA) and a graphite monochromator in the 2θ range of 20–80°. Scanning electron microscopy (SEM; JEOL JSM-6500F) was utilized to elucidate the microstructures of the specimens. The apparent densities of the specimens were measured using the Archimedes method using distilled water.

The microwave dielectric properties of the specimens were measured using the postresonator method that was developed by Hakki and Coleman [5]. The postresonator scheme utilized a specimen in the form of a cylinder of diameter D and length L. The specimens whose microwave dielectric property was measured had an aspect ratio D/L of approximately 1.6, which is in the range identified as acceptable by Kobayashi and Katoh [6]. The cylindrical resonator was sandwiched between two conducting plates. Two small antennas were positioned in the vicinity of the specimen to couple the microwave signal power into or out of the resonator. The other ends of the antennas were connected to an Agilent E5071C network analyzer. The resonance characteristics depended on the size and dielectric properties of the specimen. The microwave energy was coupled using electric-field probes. The TE_{011}

---

* Tel.: +886 2 8209 3211x5541; fax: +886 2 82099721.
E-mail addresses: EE049@mail.lhu.edu.tw, ycchenncku@yahoo.com.tw

0925-8388/$ – see front matter © 2012 Elsevier B.V. All rights reserved.
doi:10.1016/j.jallcom.2012.03.015

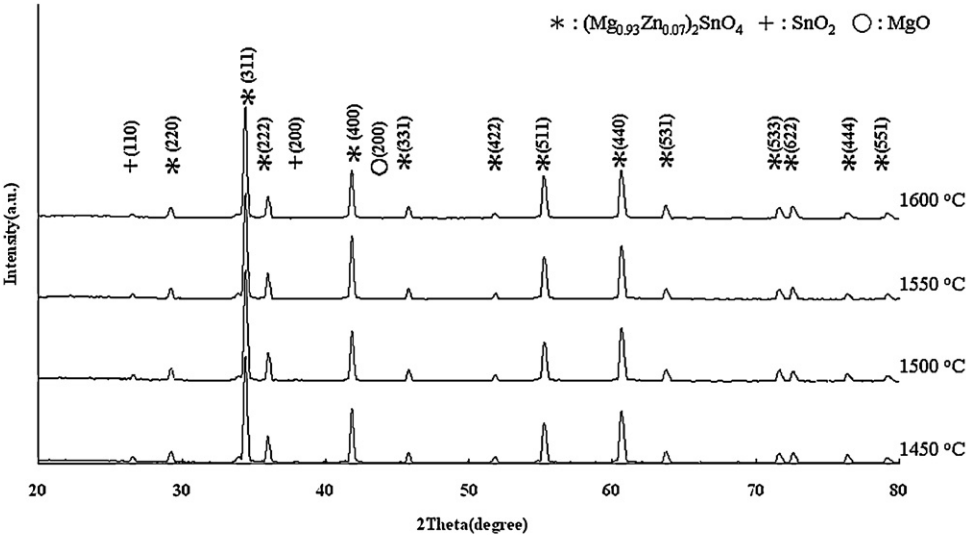

Fig. 1. X-ray diffraction patterns of $(Mg_{0.93}Zn_{0.07})_2SnO_4$ specimens sintered at 1450–1600 °C for 4 h.

resonant mode was optimal for determining the dielectric constant and the loss factor of the specimen. The Agilent E5071C network analyzer was used to identify the TE_{011} resonant frequency of the dielectric resonator, and the dielectric constant and quality factor were calculated. The scheme for measuring τ_f was the same as that for measuring the dielectric constant. The test cavity was placed in a chamber and the temperature was increased from 25 to 75 °C. The τ_f value (ppm/°C) was determined by noting the change in resonant frequency,

$$\tau_f = \frac{f_2 - f_1}{f_1(T_2 - T_1)}, \tag{1}$$

where f_1 and f_2 represent the resonant frequencies at T_1 and T_2, respectively.

3. Results and discussion

Fig. 1 displays the X-ray diffraction patterns of $(Mg_{0.93}Zn_{0.07})_2SnO_4$ ceramics that were sintered at 1450–1600 °C for 4 h. Clearly, $(Mg_{0.93}Zn_{0.07})_2SnO_4$ is the main crystalline phase, which is accompanied by small amounts of MgO and SnO_2 as secondary phases, indicating that some of the $MgSnO_3$ might have formed in the initial stages. The parallel reactions are as follows:

$$MgO + SnO_2 \rightarrow MgSnO_3, \tag{2}$$

and

$$2MgO + SnO_2 \rightarrow Mg_2SnO_4, \tag{3}$$

$MgSnO_3$ is unstable at high temperatures and thermally decomposes into Mg_2SnO_4 and SnO_2.

$$MgSnO_3 \rightarrow 0.5Mg_2SnO_4 + 0.5SnO_2, \tag{4}$$

These results are consistent with those of Pfaff [7]. The SnO_2 intensity decreased at high sintering temperature, revealing evaporation of SnO_2 at high temperatures according to the reaction [8]:

$$SnO_2(s) \rightarrow SnO(g) + 0.5O_2(g), \tag{5}$$

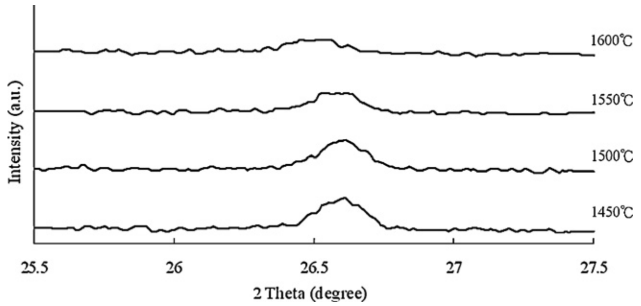

Fig. 2. X-ray diffraction patterns of $(Mg_{0.93}Zn_{0.07})_2SnO_4$ ceramics in the 2θ range of 25.5–27.5° that were sintered at 1400–1550 °C for 4 h.

Figs. 2 and 3 show the X-ray diffraction patterns of the $(Mg_{0.93}Zn_{0.07})_2SnO_4$ ceramics in the 2θ range of 25.5–27.5° and 42.6–43.0° that were sintered at 1450–1600 °C for 4 h. The amount of SnO_2 decreased with increasing sintering temperature. The relative integrated intensities demonstrated the difference in amounts of $(Mg_{0.93}Zn_{0.07})_2SnO_4$, SnO_2, and MgO more clearly [9]. The relative integrated densities can be assumed to be represented the amount of phases presented. The relative integrated intensities of $(Mg_{0.93}Zn_{0.07})_2SnO_4$, SnO_2, and MgO were evaluated from most intensive lines of each phase. For example, the relative integrated intensity of $(Mg_{0.93}Zn_{0.07})_2SnO_4$ was calculated as follows:

$$\text{Relative intensity of } (Mg_{0.93}Zn_{0.07})_2SnO_4 = \frac{I_{(Mg_{0.93}Zn_{0.07})_2SnO_4(3\,1\,1)}}{I_{(Mg_{0.93}Zn_{0.07})_2SnO_4(3\,1\,1)} + I_{SnO_2(1\,1\,0)} + I_{MgO(2\,0\,0)}} \times 100, \tag{6}$$

Table 1 shows the amount of SnO_2 decreased significantly from 5.52% to 4.20% as the sintering temperature increased from 1550 to 1600 °C, which is in agreement with Eq. (5). The variation of the amounts of $(Mg_{0.93}Zn_{0.07})_2SnO_4$ and MgO with sintering temperature was not significant compared with that of SnO_2. The formation of second phases of SnO_2 and MgO affected the microwave dielectric properties of $(Mg_{0.93}Zn_{0.07})_2SnO_4$ ceramics.

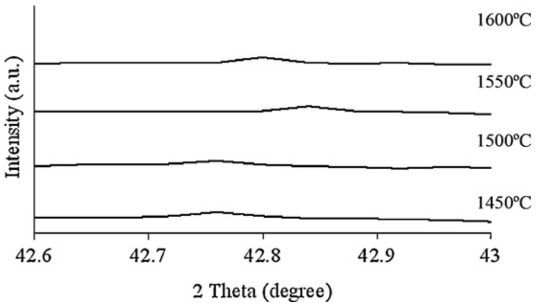

Fig. 3. X-ray diffraction patterns of $(Mg_{0.93}Zn_{0.07})_2SnO_4$ ceramics in the 2θ range of 42.6–43.0° that were sintered at 1400–1550 °C for 4 h.

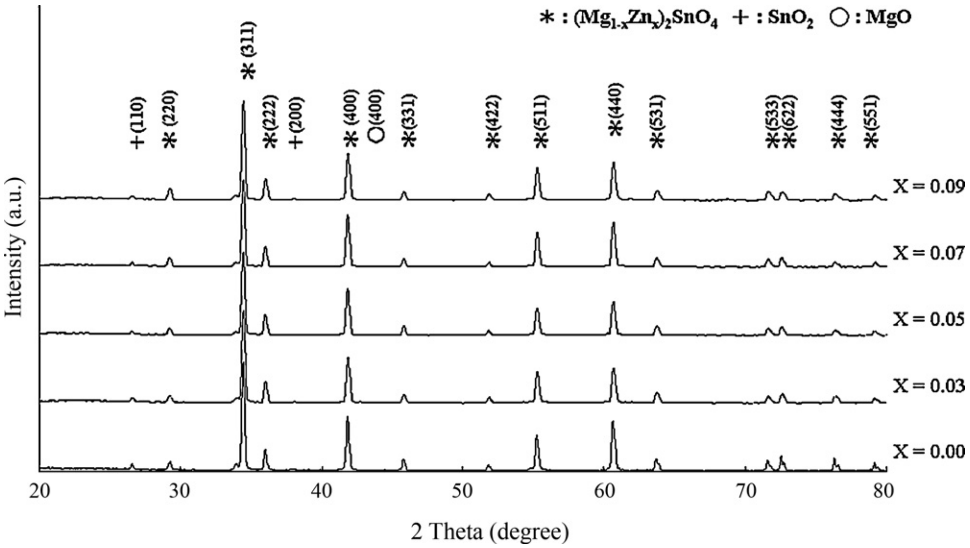

Fig. 4. X-ray diffraction patterns of $(Mg_{(1-x)}Zn_x)_2SnO_4$ ceramics with x varied from 0 to 0.09, following sintering at 1550 °C for 4 h.

Table 1
Amount of $(Mg_{0.93}Zn_{0.07})_2SnO_4$, SnO_2, and MgO of $(Mg_{0.93}Zn_{0.07})_2SnO_4$ sintered at 1450–1600 °C for 4 h.

Sintering temperature (°C)	$(Mg_{0.93}Zn_{0.07})_2SnO_4$	SnO_2 (%)	MgO (%)
1450	91.71	5.70	2.59
1500	92.40	5.76	1.84
1550	92.29	5.52	2.19
1600	93.57	4.20	2.23

Fig. 4 shows the X-ray diffraction patterns of $(Mg_{(1-x)}Zn_x)_2SnO_4$ ceramics as x varied from 0 to 0.09, following sintering at 1550 °C for 4 h. The intensity of second phases of MgO and SnO_2 did not significantly vary with the degrees of Zn^{2+} substitution. Table 2 shows the unit cell volume of $(Mg_{(1-x)}Zn_x)_2SnO_4$ ceramics as x increased from 0 to 0.09. The unit cell volume of $(Mg_{(1-x)}Zn_x)_2SnO_4$ ceramics increased from 644.41 to 647.60 Å^3 as x increased from 0 to 0.09.

Fig. 5 shows the microstructures of $(Mg_{(1-x)}Zn_x)_2SnO_4$ following sintering for 4 h at different temperatures. The microstructures of $(Mg_{(1-x)}Zn_x)_2SnO_4$ ceramics when Mg^{2+} ions were replaced with different extent of Zn^{2+} substitution indicated that the average grain size did not vary significantly with x varied from 0 to 0.09. The $(Mg_{0.93}Zn_{0.07})_2SnO_4$ ceramics were not dense, and grains did not grow after sintering at 1450 °C for 4 h, potentially degrading the microwave dielectric properties of the $(Mg_{0.93}Zn_{0.07})_2SnO_4$ ceramics. Comparing the microstructures of $(Mg_{0.93}Zn_{0.07})_2SnO_4$ ceramics that were sintered under different temperatures indicated that the average grain size increased as sintering temperature increased from 1450 to 1600 °C. However, porous microstructures occurred at high sintering temperature (1600 °C).

Fig. 6 shows the apparent densities of $(Mg_{(1-x)}Zn_x)_2SnO_4$ ceramics with different degrees of Zn^{2+} substitution, following sintering at 1450–1600 °C for 4 h. The apparent density of $(Mg_{0.93}Zn_{0.07})_2SnO_4$ ceramics that were sintered at 1450–1600 °C for 4 h was highest, 4.74 g/cm^3, when sintering was conducted at 1550 °C, beyond which temperature, it declined. The increase in apparent density may be caused by the decrease in the number of pores and the decrease in apparent density may be caused by the porous microstructure, as presented in Fig. 3. The maximum apparent density of $(Mg_{(1-x)}Zn_x)_2SnO_4$ ceramics increased from 4.62 to 4.80 g/cm^3 as x increased from 0 to 0.09. The increase in apparent density is associated with the fact that the Zn atom has a larger mass than the Mg atom.

Table 2
Unit cell volumes, internal strain, and relative density of $(Mg_{(1-x)}Zn_x)_2SnO_4$ ceramics sintered at 1550 °C for 4 h.

x	Unit cell volumes (Å^3)	Internal strain ($\times 10^{-3}$)	Relative density (%)
0	644.41	5.86	96.98
0.03	646.05	3.20	97.49
0.05	646.61	3.20	97.52
0.07	646.79	2.09	97.53
0.09	647.60	2.10	97.16

Fig. 7 shows the dielectric constants of $(Mg_{(1-x)}Zn_x)_2SnO_4$ ceramics with different degrees of Zn^{2+} substitution, following sintering at 1450–1600 °C for 4 h. $(Mg_{0.93}Zn_{0.07})_2SnO_4$ ceramics that were sintered at 1550 °C for 4 h had a maximum dielectric constant of 8.50. A high sintering temperature was not necessary for obtaining a high dielectric constant. The decrease in dielectric constant was associated with low apparent densities of the ceramics. A higher density is associated with lower porosity, and, therefore, a higher dielectric constant. The dielectric constant increased from 8.41 to 8.54 as x increased from 0 to 0.09 when the $(Mg_{(1-x)}Zn_x)_2SnO_4$ ceramics were sintered at 1550 °C for 4 h. The fact might be explained by the ionic polarization. The dielectric constant can be calculated using the Clausius–Mossotti equation, as suggested by Tohdo et al. [10]:

$$\varepsilon_r = \frac{3V_m + 8\pi\alpha_D}{3V_m - 4\pi\alpha_D}, \tag{7}$$

where V_m is the molar volume, α_D is the sum of ionic polarizations of individual ions. The dielectric constant calculated by Eq. (7) was intrinsic factor to dielectric property. Dielectric constants therefore depend on the molar volume and the ionic polarization. As seen from Eq. (7), a smaller molar volume or a larger ionic polarization, is associated with a larger obtained dielectric constant. The influence of ionic polarization on dielectric constant is much larger than that of molar volume. The ionic polarization of Zn^{2+} ion and Mg^{2+} ion are 2.04 and 1.32 Å^3, respectively [11,12]. The sum of ionic polarization of $(Mg_{(1-x)}Zn_x)_2SnO_4$ ceramics increased as x increased, so the dielectric constant of $(Mg_{(1-x)}Zn_x)_2SnO_4$ ceramics increased as x increased.

Fig. 8 shows the $Q \times f$ of the $(Mg_{(1-x)}Zn_x)_2SnO_4$ ceramics with different degrees of Zn^{2+} substitution, following sintering at 1450–1600 °C for 4 h. $(Mg_{(1-x)}Zn_x)_2SnO_4$ ceramics that were sintered at 1550 °C for 4 h had the highest $Q \times f$ of 186,100 GHz. The

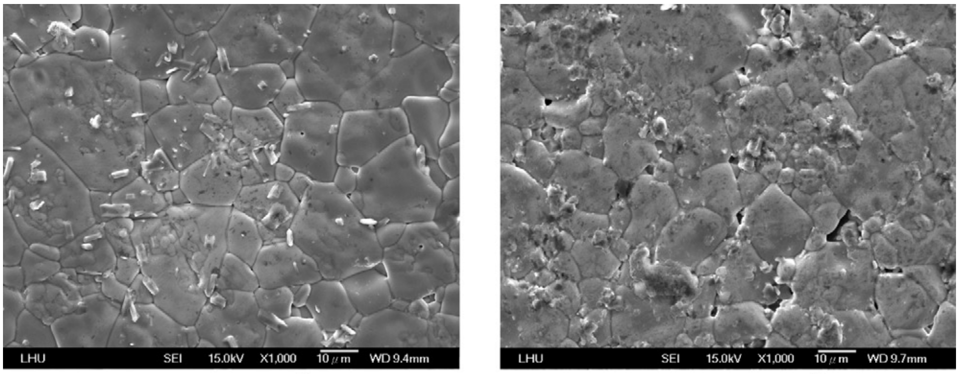

(a) x=0, 1550 ^{O}C (b) x=0.03, 1550 ^{O}C

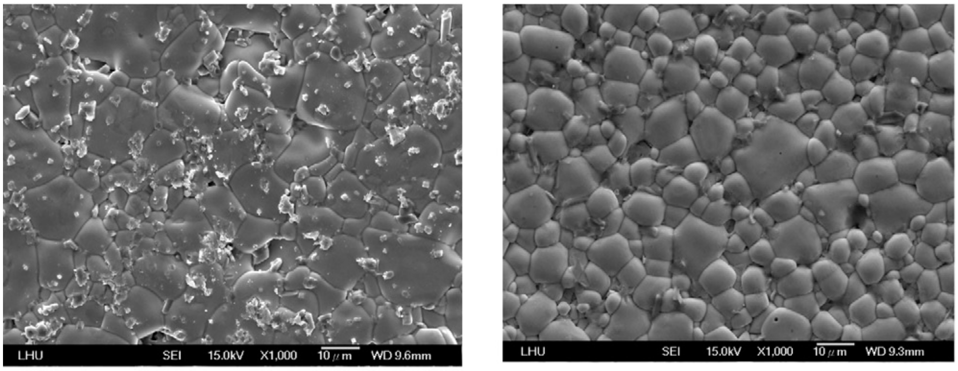

(c) x=0.05, 1550 ^{O}C (d) x=0.07, 1450 ^{O}C

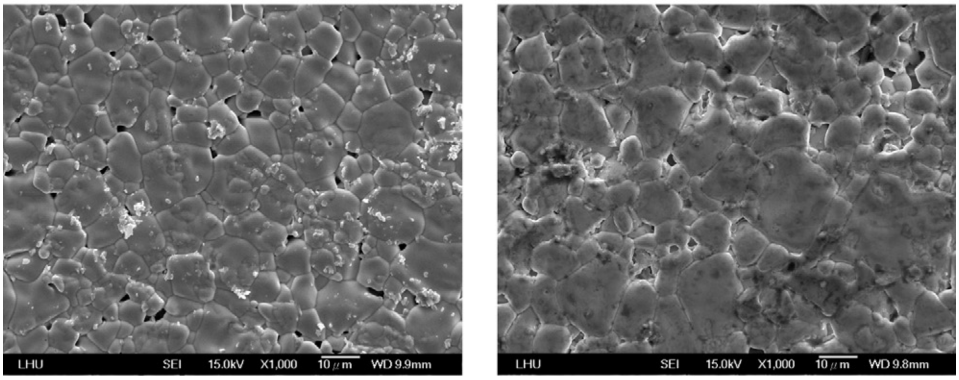

(e) x=0.07, 1500 ^{O}C (f) x=0.07, 1550 ^{O}C

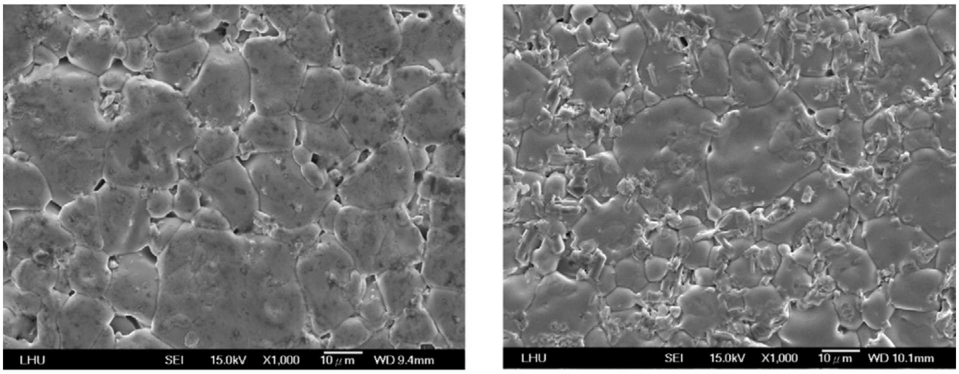

(g) x=0.07, 1600 ^{O}C (h) x=0.09, 1550 ^{O}C

Fig. 5. Microstructures of $(Mg_{(1-x)}Zn_x)_2SnO_4$ ceramics sintered under different temperatures for 4 h: (a) $x = 0/1550\,^{\circ}C$, (b) $x = 0.03/1550\,^{\circ}C$, (c) $x = 0.05/1550\,^{\circ}C$, (d) $x = 0.07/1450\,^{\circ}C$, (e) $x = 0.07/1500\,^{\circ}C$, (f) $x = 0.07/1550\,^{\circ}C$, (g) $x = 0.07/1600\,^{\circ}C$, and (h) $x = 0.09/1550\,^{\circ}C$.

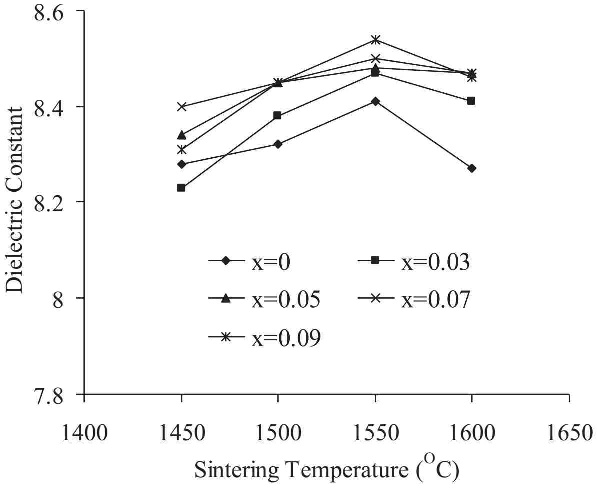

Fig. 6. Apparent densities of $(Mg_{(1-x)}Zn_x)_2SnO_4$ ceramics with different degrees of Zn^{2+} substitution, following sintering at different temperatures for 4 h.

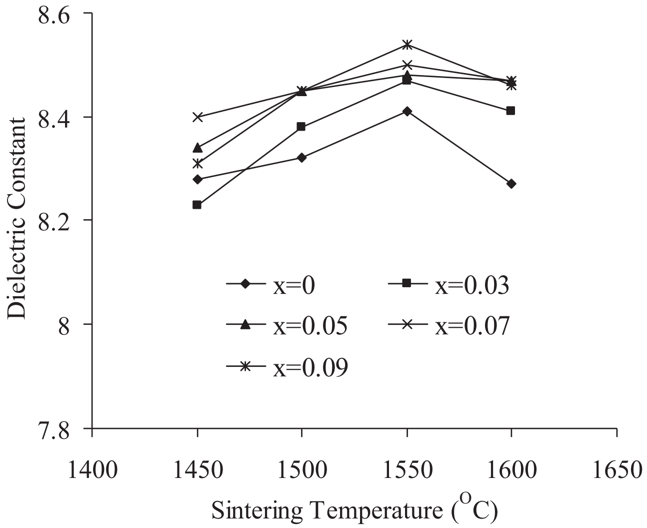

Fig. 7. Dielectric constants of $(Mg_{(1-x)}Zn_x)_2SnO_4$ ceramics with different degrees of Zn^{2+} substitution, following sintering at different temperatures for 4 h.

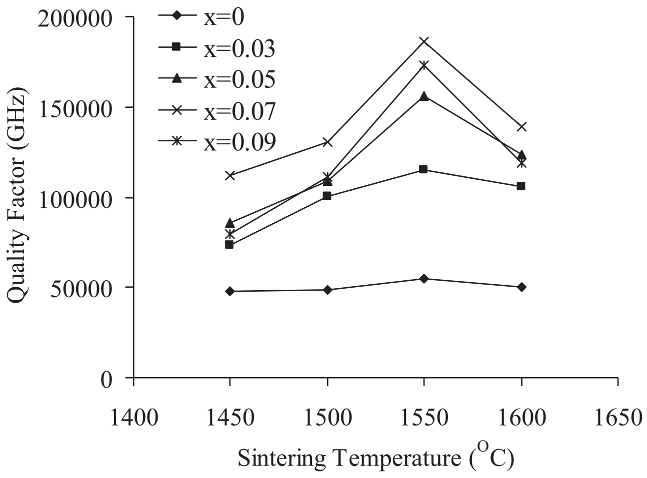

Fig. 8. $Q \times f$ of $(Mg_{(1-x)}Zn_x)_2SnO_4$ ceramics with different degrees of Zn^{2+} substitution, following sintering at different temperatures for 4 h.

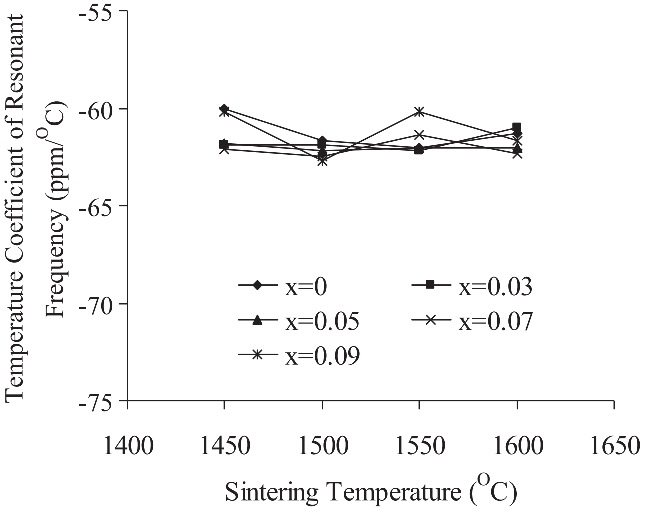

Fig. 9. τ_f of $(Mg_{(1-x)}Zn_x)_2SnO_4$ ceramics with different degrees of Zn^{2+} substitution, following sintering at different temperatures for 4 h.

relationship between the $Q \times f$ and the sintering temperature was consistent with that between the apparent density and the sintering temperature, because the microwave dielectric loss was affected by many factors, and consisted of intrinsic and extrinsic components. Intrinsic loss is associated with the lattice vibrational modes. Extrinsic loss is related to the density, porosity, second phases, impurities, oxygen vacancies, grain size, internal strain, and lattice defects [13,14]. Since the $Q \times f$ of $(Mg_{0.93}Zn_{0.07})_2SnO_4$ ceramics was consistent with the variation of the apparent density, it is suggested to be dominated by the apparent density. The $Q \times f$ increased from 55,000 to 186,100 GHz as x increased from 0 to 0.07, then decreased from 186,100 to 173,000 GHz as x increased from 0.07 to 0.09, when the $(Mg_{(1-x)}Zn_x)_2SnO_4$ ceramics were sintered at 1550 °C for 4 h. This was associated with the internal strain and density. The internal strain η can be calculated by following equation, as suggested by Ohsato and Imaeda [15].

$$\beta = 2\eta \tan\theta, \tag{8}$$

where β is the full width at half maximum (FWHM) of X-ray diffraction peaks, θ is the diffraction angles. The grain size is also a factor that will affect FWHM of the specimen. Since the average grain size did not vary significantly with the extent of Zn^{2+} substitution, curve fitting was used to fit the internal strain η of $(Mg_{(1-x)}Zn_x)_2SnO_4$ ceramics with different degrees of Zn^{2+} substitution with Eq. (8). The curve fittings were based on the least-squares method. In this method, the square of the deviation of the experimental value from the theoretical expectation was calculated while varying the fitted internal strain. The fitting process was ended at a specific value of the fitted internal strain where the deviation was minimized.

The low internal strain associated with the ordering distribution of the ions, therefore, resulted in a high quality factor. There are similar examples in other microwave ceramic materials [16,17]. The $La(Mg_{0.5-x}Ca_xSn_{0.5})O_3$ and $La_{1-x}Bi_x(Mg_{0.5}Sn_{0.5})O_3$ ceramics exhibited excellent quality factor as they had low internal strain. As shown in Table 2, the internal strain of $(Mg_{0.93}Zn_{0.07})_2SnO_4$ ceramics is lowest, then the $Q \times f$ of $(Mg_{0.93}Zn_{0.07})_2SnO_4$ ceramics is largest. In the second case of density, the relative density increased from 96.98% to 97.53% as x increased from 0 to 0.07, then decreased from 97.53% to 97.16% as x increased from 0.07 to 0.09 as shown in Table 2. Densification plays an important role in controlling the $Q \times f$ as described above.

Fig. 9 shows the temperature coefficient of resonant frequency (τ_f) of $(Mg_{(1-x)}Zn_x)_2SnO_4$ ceramics with different degrees of Zn^{2+}

substitution, following sintering at 1450–1600 °C for 4 h. Generally, τ_f is related to the composition, the amount of additive, and the second phases that are present in the ceramics. Although second phases of MgO and SnO_2 were found, variation of the amount of second phases with x was not significant, which the influence on the τ_f of $(Mg_{(1-x)}Zn_x)_2SnO_4$ ceramics, was small. Since the composition of $(Mg_{(1-x)}Zn_x)_2SnO_4$ ceramics with a fixed amount of Zn^{2+} substitution did not vary with sintering temperature, no significant variation in τ_f of $(Mg_{(1-x)}Zn_x)_2SnO_4$ ceramics with sintering temperature over the entire range of sintering temperatures considered herein was observed. A τ_f of −61 ppm/°C was measured for $(Mg_{0.93}Zn_{0.07})_2SnO_4$ ceramics that were sintered at 1550 °C for 4 h. Relatively high τ_f of the $(Mg_{0.93}Zn_{0.07})_2SnO_4$ ceramics precludes its immediate application potential. A later investigation will involve tailoring the τ_f of $(Mg_{0.93}Zn_{0.07})_2SnO_4$ ceramics.

4. Conclusions

The effects of the degree of Zn^{2+} substitution and sintering temperature on the microwave dielectric properties of $(Mg_{(1-x)}Zn_x)_2SnO_4$ ceramics were studied. The microwave dielectric properties of $(Mg_{(1-x)}Zn_x)_2SnO_4$ ceramics were improved by substituting Mg^{2+} ions with Zn^{2+} ions. The X-ray diffraction peaks of $(Mg_{0.93}Zn_{0.07})_2SnO_4$ ceramics did not vary significantly with sintering temperatures. $(Mg_{0.93}Zn_{0.07})_2SnO_4$ ceramics that were sintered at 1550 °C for 4 h had an apparent density of 4.74 g/cm^3, a dielectric constant of 8.50, a $Q \times f$ of 186,100 GHz, and a temperature coefficient of resonant frequency (τ_f) of −61 ppm/°C. The dielectric constant of $(Mg_{(1-x)}Zn_x)_2SnO_4$ ceramics was affected by the density and ionic polarization. The $Q \times f$ of $(Mg_{(1-x)}Zn_x)_2SnO_4$ ceramics depended on the density and internal strain.

Acknowledgments

The authors would like to thank the National Science Council in Taiwan for financially supporting this research under Contract No. NSC 100-2622-E-262-001-CC3.

References

[1] Y.B. Chen, J. Alloys Compd. 509 (2011) 1050–1053.
[2] Y.B. Chen, J. Alloys Compd. 509 (2011) 6884–6888.
[3] Y.C. Chen, Y.N. Wang, C.H. Hsu, J. Alloys Compd. 509 (2011) 9650–9653.
[4] R.D. Shannon, Acta Crystallogr. A 32 (1976) 751–767.
[5] B.W. Hakki, P.D. Coleman, IEEE Trans. Microw. Theory Tech. 8 (1960) 402–410.
[6] Y. Kobayashi, M. Katoh, IEEE Trans. Microw. Theory Tech. 33 (1985) 586–592.
[7] G. Pfaff, Thermochim. Acta 237 (1994) 83–90.
[8] E.R. Leite, J.A. Cerri, E. Longo, J.A. Varela, C.A. Paskocima, J. Eur. Ceram. Soc. 21 (2001) 669–675.
[9] S.P. Wu, J.H. Luo, J. Alloys Compd. 509 (2011) 8126–8132.
[10] Y. Tohdo, K. Kakimoto, H. Ohsato, H. Yamada, T. Okawa, J. Eur. Ceram. Soc. 26 (2006) 2039–2043.
[11] R.D. Shannon, J. Appl. Phys. 73 (1993) 348–366.
[12] C. Veneis, P.K. Davies, T. Negas, S. Bell, Mater. Res. Bull. 31 (1996) 431–437.
[13] B.D. Silverman, Phys. Rev. 125 (1962) 1921–1930.
[14] W.S. Kim, T.H. Hong, E.S. Kim, K.H. Yoon, Jpn. J. Appl. Phys. 37 (1998) 3567–3571.
[15] H. Ohsato, M. Imaeda, Mater. Chem. Phys. 79 (2003) 208–212.
[16] Y.C. Chen, M.D. Chen, J. Phys. Chem. Solids 72 (2011) 1447–1451.
[17] Y.C. Chen, W.C. Lee, Mater. Chem. Phys. 129 (2011) 1110–1115.